JCB Article

Toxoplasma gondii myosins B/C: one gene, two tails, two localizations, and a role in parasite division

Frédéric Delbac,[1,2] Astrid Sänger,[1] Eva M. Neuhaus,[3] Rolf Stratmann,[1] James W. Ajioka,[4] Catherine Toursel,[5] Angelika Herm-Götz,[1] Stanislas Tomavo,[5] Thierry Soldati,[3] and Dominique Soldati[1]

[1]Zentrum für Molekulare Biologie, Universität Heidelberg, D-69120 Heidelberg, Germany
[2]Laboratoire de Biologie des Protistes, Centre National de la Recherche Scientifique (CNRS), UMR 6023, Université Blaise Pascal, 63177 Aubière, France
[3]Department of Molecular Cell Research, Max Planck Institute for Medical Research, D-69120 Heidelberg, Germany
[4] Department of Pathology, University of Cambridge, Cambridge CB2 1QP, United Kingdom
[5]UMR CNRS 8576 Université des Sciences et Technologies de Lille, France

In apicomplexan parasites, actin-disrupting drugs and the inhibitor of myosin heavy chain ATPase, 2,3-butanedione monoxime, have been shown to interfere with host cell invasion by inhibiting parasite gliding motility. We report here that the actomyosin system of *Toxoplasma gondii* also contributes to the process of cell division by ensuring accurate budding of daughter cells. *T. gondii* myosins B and C are encoded by alternatively spliced mRNAs and differ only in their COOH-terminal tails. MyoB and MyoC showed distinct subcellular localizations and dissimilar solubilities, which were conferred by their tails. MyoC is the first marker selectively concentrated at the anterior and posterior polar rings of the inner membrane complex, structures that play a key role in cell shape integrity during daughter cell biogenesis. When transiently expressed, MyoB, MyoC, as well as the common motor domain lacking the tail did not distribute evenly between daughter cells, suggesting some impairment in proper segregation. Stable overexpression of MyoB caused a significant defect in parasite cell division, leading to the formation of extensive residual bodies, a substantial delay in replication, and loss of acute virulence in mice. Altogether, these observations suggest that MyoB/C products play a role in proper daughter cell budding and separation.

Introduction

The actin cytoskeleton plays a fundamental role in host cell invasion by apicomplexan parasites (Dobrowolski and Sibley, 1997; Pinder et al., 1998, 2000). In *Toxoplasma gondii*, in particular, motility and host cell invasion are powered by the parasite actin cytoskeleton and most likely by myosin motors (Dobrowolski and Sibley, 1996). A recent report established the essential role of microtubules during parasite division and shed light on a distinct role of the actin cytoskeleton: contributing to proper inheritance of organelles into daughter cells (Shaw et al., 2000). Both microtubule and actin cytoskeletons are essential components of the machineries responsible for genome segregation and cell division in eukaryotes (Field et al., 1999; Goode et al., 2000). Conventional class II myosins contribute to force production by driving cleavage furrow contractility, an essential process during separation of daughter cells (Robinson and Spudich, 2000; for review see Bezanilla et al., 2000). Recently, two unconventional myosins of class V have been implicated in *Schizosaccharomyces pombe* cytokinesis (Win et al., 2001). In apicomplexan parasites, nuclear division occurs by endomitosis, a cytokinetic process without nuclear membrane breakdown. As in other organisms, microtubules play a key role during replication, when the ends of microtubules are inserted into the nuclear envelope at the spindle body (Tilney and Tilney, 1996; Shaw et al., 2000). In *T. gondii*, cytokinesis involves the internal budding of two daughter cells from the common cytoplasmic mass of the parental cell by a mechanism called endodyogeny (Fig. 1; Vivier and Petitprez, 1969). In other apicomplexa such as *Theileria*, four cells bud from the common cytoplasmic mass, and in *Plasmodium* species, four nuclear divisions occur before the budding of 16 daughter cells. This mode of division

Address correspondence to Dr. Dominique Soldati, Department of Biological Sciences, Imperial College of Science, Technology, and Medicine, Imperial College Road, London SW7 2AZ, United Kingdom. Tel.: (44) 207-594-5342. Fax: (44) 207-584-2056. E-mail: d.soldati@ic.ac.uk

F. Delbac and A. Sänger contributed equally to these studies.

D. Soldati, T. Soldati, and R. Stratmann's present address is Department of Biological Sciences, Imperial College of Science, Technology, and Medicine, London SW7 2AZ, United Kingdom.

Key words: Apicomplexa; unconventional myosin XIV; localization; *Toxoplasma gondii*; cell division

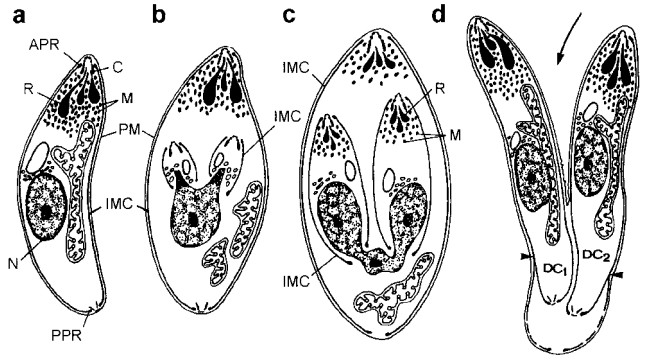

Figure 1. **Endodyogeny in *T. gondii*.** Schematic representation of the different stages of division within a mother cell (adapted from Kepka and Scholtyseck, 1970; *Frankelia* species). Cell division starts with the formation of the two daughter conoids, the IMCs, and the microtubule baskets (b). It is followed by the entrapment of the apical secretory organelles, micronemes, and rhoptries (c). The IMC of the mother cell (a) somehow gives rise to the daughter cells' membrane complexes, which progress toward the posterior pole while the nucleus divides. Final separation occurs by budding through the mother cell plasma membrane and by constriction at the posterior end (d). APR, apical polar ring; C, conoid; M, micronemes; N, nucleus; PM, plasma membrane; PPR, posterior polar ring; R, rhoptries.

is called merogony or schizogony. It is essential that each newly formed cell receives one nucleus, one mitochondrion, a Golgi apparatus, some rough endoplasmic reticulum, and a few copies of each specialized organelle necessary to invade the next host cell. Closely apposed to the plasma membrane, a series of flat cisternae constitute the inner membrane complex (IMC).* Budding proceeds concomitantly with the formation of the IMC and a basket of circumferentially arranged microtubules that extend from the polar ring surrounding the apical prominence. An intramembranous particle lattice within the IMC is associated with the subpellicular microtubules, likely contributing to shape maintenance and dynamics of the parasite (Morrissette et al., 1997).

The current repertoire of myosins in *T. gondii* is comprised of four genes giving rise to five distinct proteins, all of the class XIV, which appears restricted to members of the Apicomplexa phylum (Heintzelman and Schwartzman, 2001). In a previous study, we showed that endogenous MyoA localizes beneath the plasma membrane, and that its short tail carries the localization determinant (Hettmann et al., 2000), making MyoA an appealing candidate for power gliding motility. Nothing is known yet about the function of the other myosins. MyoB and MyoC are encoded by a single gene that gives rise to two alternatively spliced mRNAs, which encode two myosins with distinct tails (Heintzelman and Schwartzman, 1997). MyoC has been recently reported to localize to a structure reminiscent of the Golgi apparatus (Heintzelman and Schwartzman, 1999). In the closely related parasite *Plasmodium falciparum*, three myosins have been reported so far. PfMyoA and PfMyoB also belong to the class XIV and are structurally very similar to *T. gondii* MyoA, whereas PfMyoC is a larger, unclassified myosin.

Here, we report about the determination of the expression pattern of MyoB/C products and the predominant role of their tails in subcellular localization. The cellular distribution and phenotypes resulting from the overexpression of wild-type or mutant forms of MyoB and MyoC strongly suggest that the MyoB/C gene products are implicated in parasite division.

Results

T. gondii myosins are differentially regulated between the tachyzoite and bradyzoite stages

Treatment of intracellular parasites with actin inhibitors was reported to have marginal effects on parasite growth and replication, but induced the formation of large residual bodies at the posterior end of dividing parasites (Shaw et al., 2000). In preliminary experiments, treatment with the myosin heavy chain ATPase inhibitor, 2,3-butanedione monoxime (BDM), induced a significant replication delay and the formation of enlarged parasites that failed to accomplish proper cell division (unpublished data). EM revealed that most parasites failed to achieve proper separation, despite normal nuclear duplication and acquisition of individual organelles, including the conoid and the nascent IMC. The effect of BDM was suggestive of a role for myosin(s) in cell division, but was nevertheless inconclusive because of the risk that BDM may have affected a nonmyosin target.

Toward the identification of a myosin contributing to cell division, we analyzed the pattern of expression of the five known myosins in the two invasive life stage forms of *T. gondii* present in intermediate hosts. Specific transcripts coding for myosins A, B, C, and D (not shown), but not E, were amplified by RT-PCR using total RNAs isolated from the rapidly replicating tachyzoites (Fig. 2 A). Furthermore, a comparison of the amount of specific transcripts between tachyzoites and the dormant, encysted bradyzoites was assessed by semiquantitative RT-PCR (Fig. 2 B), as previously described (Yahiaoui et al., 1999). Rather unexpectedly and with the exception of MyoA, the myosin mRNAs were more abundant in the persistent stage. This analysis did not distinguish between the increased rate of transcription and the increased stability of transcripts in bradyzoites compared with tachyzoites. Expressed sequence tag (EST) clones corresponding to myosins are extremely underrepresented in the 10,000 ESTs found in the *T. gondii* database (Ajioka et al., 1998). Nevertheless, the same tendency toward a predominant representation in bradyzoite compared with tachyzoite cDNAs was observed (http://www.cbil.upenn.edu/ParaDBs/). Indeed, 11 EST clones specific for MyoC were present in the in vivo bradyzoite cDNA library compared with two ESTs in the much larger pool of *T. gondii* RH strain tachyzoite ESTs. This imbalance reflects and strengthens the results obtained by RT-PCR. The two transcripts encoding MyoB and MyoC were previously described and presumed to derive from alternative RNA splicing (Heintzelman and Schwartzman, 1997).

To investigate the expression of MyoB and MyoC, we raised polyclonal antipeptide sera specific to each protein and to MyoB/C. The COOH-terminal peptide of 21 resi-

*Abbreviations used in this paper: BDM, 2,3-butanedione monoxime; EST, expressed sequence tag; GFP, green fluorescence protein; HFF, human foreskin fibroblast; HXGPRT, hypoxanthine-xanthine-guanine-phosphoribosyltransferase; IFA, immunofluorescence assay; IMC, inner membrane complex; UTR, untranslated region.

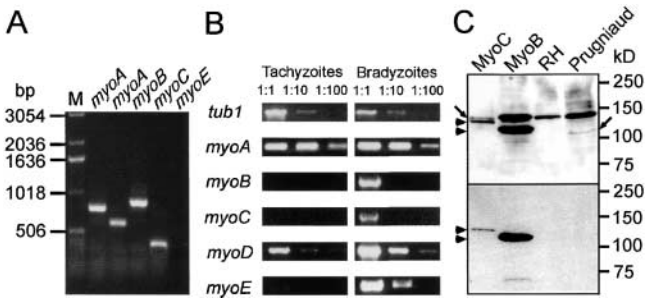

Figure 2. **Comparison of the expression of *T. gondii* myosin transcripts and proteins between tachyzoites and bradyzoites.** (A) RT-PCR amplification of *T. gondii* myosin transcripts from total tachyzoite RNA with two distinct sets of primers specific to MyoA and one set of primers specific for MyoB, MyoC, and MyoE. (B) Semi-quantitative RT-PCR analysis on total RNA prepared from tachyzoites cultivated in vitro and bradyzoites encysted in vivo. After first strand synthesis, the cDNAs of MyoA, MyoB, MyoC, MyoD, and MyoE, as well as the tubulin mRNA, TUB1 (used as a control), were detected using appropriate primer pairs. Serial dilutions of the cDNAs were 1:10 and 1:100. The size of the PCR products were as expected from the respective cDNA sequence. (C) Western blot analysis of lysates prepared from extracellular RH, the persistent strain Prugniaud, RHMyoC, and RHMyoB. In the upper half, the membrane was incubated with the antiserum raised against peptides B/C1 and B/C2. The monoclonal anti-myc was used in the lower half.

dues specific to MyoB has poor predicted antigenicity, and sera raised against it failed to detect MyoB (unpublished data). In Western blots, a sera raised against bacterially expressed glutathione-*S*-transferase fused to the last 118 residues specific to MyoC detected a protein of the expected molecular mass of 132 kD in tachyzoites (unpublished data). Additionally, two peptides corresponding to MyoB/C (B/C1 and B/C2) and two peptides specific for MyoC (C1 and C2) were used. The corresponding antisera were affinity purified against the peptides. Fig. 2 C illustrates the detection of MyoB and MyoC in freshly released parasites from RH and Prugniaud strains with a serum raised against MyoB/C peptides. No signal was detectable in the host cell lysate (unpublished data). We also transfected parasites with vectors expressing the NH_2 terminally epitope-tagged MyoB or MyoC under the control of the constitutive TUB1 promoter. These and other expression vectors used in this study are depicted schematically in Fig. 3 C. Western blot analysis of lysates from transgenic parasites expressing myc–MyoB and myc–MyoC (Fig. 2 C, arrowheads) confirmed that both proteins are detectable with anti-MyoB/C and anti-myc antibodies. MyoC is expressed in wild-type tachyzoites (Fig 2 C, arrow on the left) as previously reported (Heintzelman and Schwartzman, 1999), whereas MyoB is apparently not detected in RH and only barely detectable in the Prugniaud strain (arrow on the right).

The MyoB/C gene generates two transcripts by alternative splicing of the last intron

To identify the mechanism generating the alternatively spliced mRNAs, we isolated and sequenced cosmid clones containing the MyoB/C locus. The genomic sequence revealed that the MyoB mRNA is derived from a larger

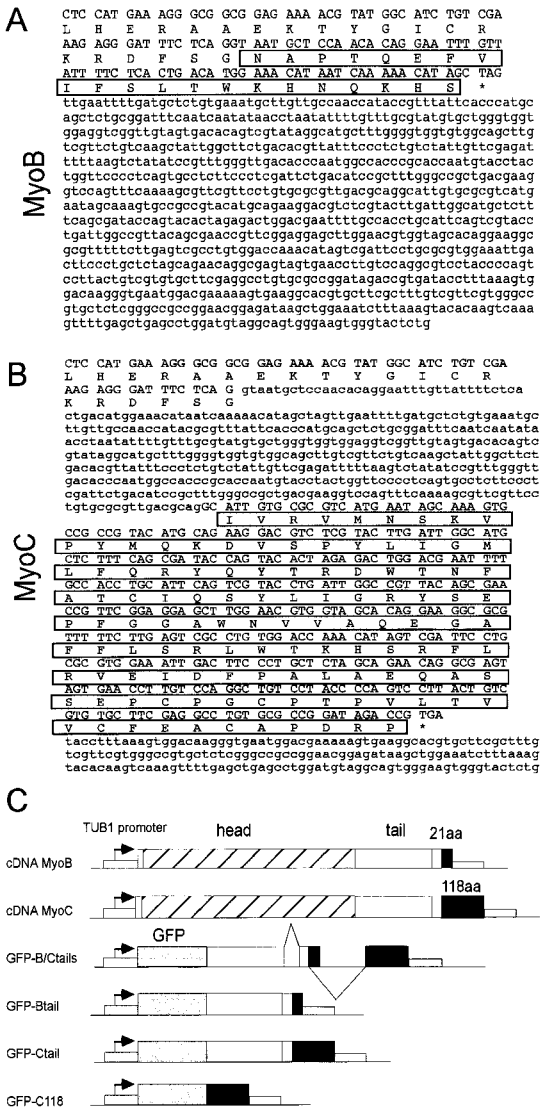

Figure 3. **The *T. gondii* MyoB/C gene is alternatively spliced to produce the two class XIV myosins B and C.** (A and B) Sequences of the MyoB/C gene encompassing the two alternatively spliced COOH-terminal exons and 3′-UTR. When the last intron remains unspliced, the long transcript generates MyoB, which contains 21 specific amino acids at the COOH terminus. Splicing of the last intron produces a shorter transcript coding for MyoC, which contains 118 specific amino acids. (C) Schematic representation of some constructs used in this study. All expression vectors contain a HXGPRT selection marker controlled by the DHFR-TS flanking sequences. The expression cassette is controlled by the TUB1 promoter and SAG1 3′UTR sequences and contains a myc-7xHis tag fused after the start codon as previously described (Hettmann et al., 2000). GFP–B/C corresponds to a fusion of GFP with the genomic sequence encompassing both MyoB and MyoC coding tail exons. The different domains are not drawn to scale.

transcript with an unspliced last intron (Fig. 3 A). The MyoB transcript codes for a polypeptide 1,074 amino acids long, ending with 21 residues specific to MyoB. In contrast, if the last intron is spliced out, a shorter transcript codes for MyoC; 1,171 amino acids long, ending with 118 amino acids unique to MyoC (Fig. 3 B). Thus, MyoB is the product of an incomplete processing of the primary transcript.

Transient expression of MyoB/C gene products reveals their biased segregation between daughter cells after endodyogeny

The very low expression level of MyoB in tachyzoites and the difficulty to unambiguously determine the subcellular localization of the two alternatively spliced products prompted us to adopt an epitope tagging strategy, as used for the characterization of MyoA (Hettmann et al., 2000). In addition, transient expression of MyoB, MyoC, and the MyoB/C motor domain lacking the tail (MyoB/CΔtail) revealed unexpected features.

First, a striking asymmetry in the repartition of MyoB, MyoC, and even MyoB/CΔtail in daughter cells was apparent 24 and 48 h after transfection. Freshly lysed parasites are asynchronous and thus undergo replication at different times after transfection and host cell infection, resulting in variable numbers of strongly positive and almost negative parasites per vacuole. Likely, if the transfected parasites divided before the transgene products had accumulated, the myosins would be present in both daughter cells. In contrast, if the protein accumulated before division, it could not be distributed evenly between the daughter cells (Fig. 4 A –D in red, E and F in green). The anti-TgMIC6 was used as a control to detect all the parasites present in the vacuole. Other cotransfected cytoplasmic or organellar markers (green fluorescence protein [GFP], catalase, or MIC6) were, without exception, evenly distributed among the parasites of a given vacuole (unpublished data). The only other reported segregation defect in *T. gondii* was observed after the expression of a chimeric molecule targeted to the apicoplast, which prevented replication of the organelle in daughter cells (He et al., 2001).

Second, MyoB was nonhomogenously distributed in the parasite cytoplasm, often found at its periphery (Fig. 4, A and B, arrows) and excluded from the nucleus. In dividing parasites, MyoB was enriched in distinct structures or lamellae that appeared to extend from the periphery in between the daughter cells (Fig. 4, A and B, small arrows). A considerable accumulation of the protein was detectable at the posterior of the parasites, forming a residual body (Fig. 4, A and B**,** arrowheads). The distribution of MyoC resembled that of MyoB, including at the periphery and in the extension between dividing parasites, but concentrated additionally at the apical and posterior poles, particularly visible when protein expression was weaker (Fig. 4 D**,** small arrows). Formation of residual bodies was also observed (Fig. 4 D, panel c, arrowhead). Most importantly, MyoB/CΔtail, the motor truncated of the tail domain, normally considered to target myosins to their place of action, was also found at the periphery (best visible in parasites with lower protein levels; Fig. 4 E, arrows) and enriched in residual bodies (Fig. 4 E, arrowhead).

Although parasites stably expressing MyoB and MyoC were obtained and analyzed (see below), multiple attempts to generate stable transformants expressing MyoB/CΔtail remained unsuccessful, suggesting that the truncated form of the protein was not tolerated.

MyoB and MyoC exhibit distinct cellular localizations

To analyze more closely the localization of the MyoB/C gene products in nondividing parasites, we generated recombinants

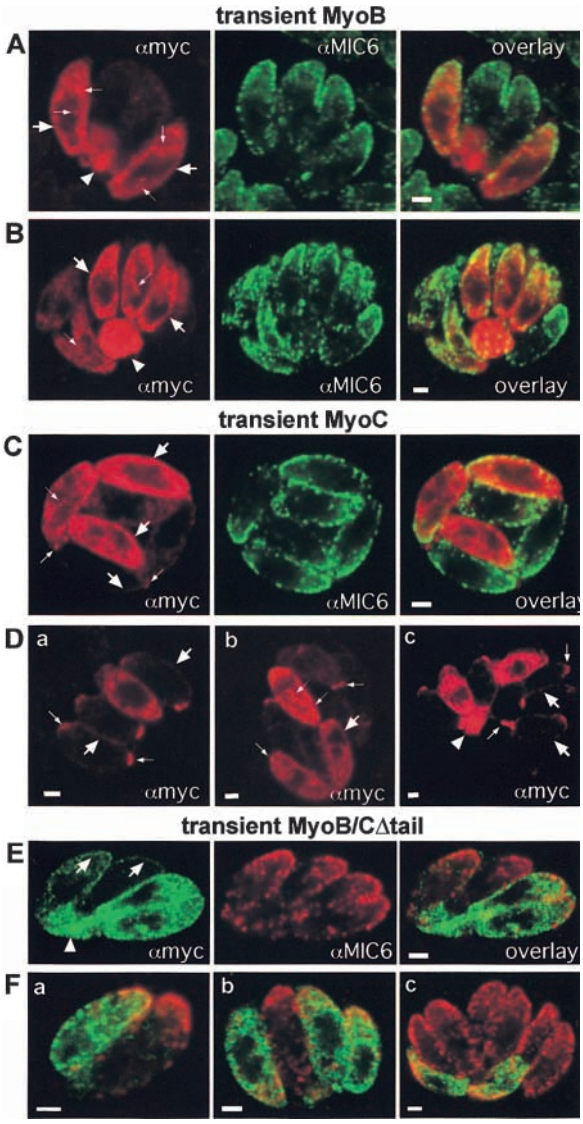

Figure 4. **Uneven segregation of MyoB/C motor proteins during cell division.** Double IFA and confocal microscopy analysis of parasites 24 h after transfection with MyoB (A and B), MyoC (C and D), or MyoB/CΔtail (E and F) constructs. Anti-MIC6 antibodies were used as markers to detect all the parasites present within a given vacuole. MyoB and MyoC (in red) and MyoB/CΔtail (in green) were detected with anti-myc antibodies. The immunofluorescence overlays showed the uneven segregation of the myosin after cell division. Transient expression of the three constructs induced the formation of residual bodies (A, B, Dc, E, arrowheads). The myosins significantly accumulated at the periphery of the cells (A–E, big arrows). In dividing parasites, MyoB (A and B) and MyoC (C and Db) were enriched in distinct structures or lamellae that appeared to extend from the periphery in between the daughter cells (small arrows). In addition, MyoC was concentrated at the poles of the parasites (C and D, small arrows). Bars, 1 μm.

stably expressing myc–MyoB or myc–MyoC. We confirmed the expression of polypeptides of the anticipated sizes by Western blotting with anti-myc antibodies (Fig. 5 C). The stably transformed parasites were then examined by immunofluorescence assay (IFA), revealing distinct, subcellular steady-state distributions (Fig. 5, A and B). As previously observed in transient transfections, MyoB was spread throughout the cytoplasm associated with a punctate structure,

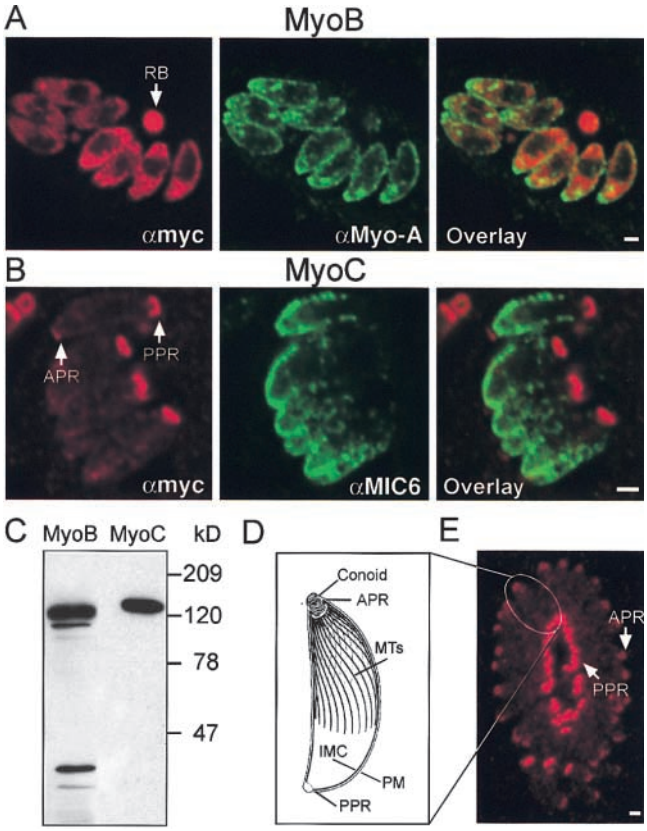

Figure 5. **Determination of the subcellular localization of MyoB and MyoC.** Transgenic parasites expressing myc–MyoB (A) or myc–MyoC (B and E) were analyzed by IFA and confocal microscopy after staining with anti-myc (A, B, and E) and either anti-MyoA (A) or anti-MIC6 (B) antibodies. MIC6 is a microneme marker defining the apical pole of the parasite. (C) Western blot analysis of parasites expressing myc–MyoB or myc–MyoC with anti-myc antibodies. (D) Schematic representation of some major morphological features of a tachyzoite (adapted from Nichols and Chiappino, 1987). (E) A parasitophorous vacuole containing a rosette of 32 tachyzoites. Note the homogeneous orientation of the parasites with their apical poles pointing outwards. APR, anterior polar ring; MTs, microtubules; PM, plasma membrane; PPR, posterior polar ring. Bars, 1 μm.

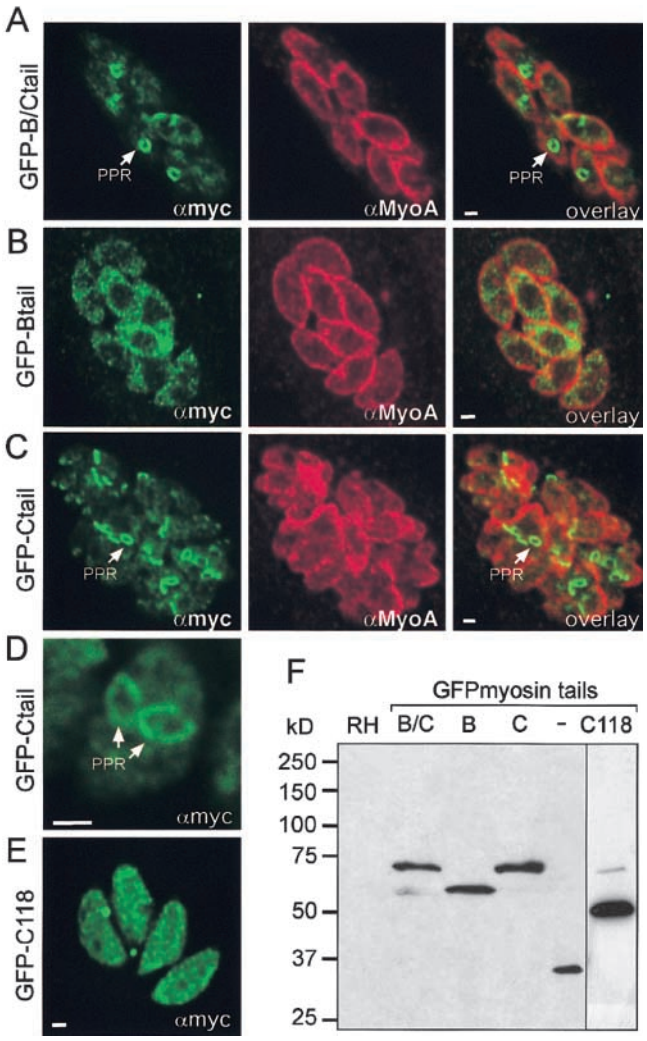

Figure 6. **Determination of the subcellular localization of GFP fusions.** (A) Transgenic parasites expressing the different GFP fusion constructs with the tails of MyoB (B), MyoC (C and D), MyoB/C (A), or the COOH-terminal 118 residues specific to MyoC (E) were analyzed by confocal immunofluorescence microscopy after staining with anti-myc (A–E) and anti-MyoA (A–C) antibodies. (D) A parasite in the process of cell division showed two ring structures in the middle of the dividing mother cell. (F) Western blot analysis of wild-type parasites (RH) and transgenic parasites expressing GFP alone, GFP–Btail, GFP–Ctail, GFP–B/Ctail, or GFP–C118. PPR, posterior polar ring. Bars, 1 μm.

whereas the distribution of MyoC was mostly restricted to the posterior and weakly to the anterior poles of the parasites (Fig. 5 E). Double immunofluorescence staining of MyoB and MyoA showed no major overlap. Additionally, the double staining against MyoC and the apical micronemal protein TgMIC6 confirmed the predominant posterior localization of MyoC. High resolution confocal microscopy distinctly identified the staining of MyoC as a ring structure, likely corresponding to the posterior polar ring and more weakly to the apical polar ring at the terminal regions of the IMC. A schematic representation of a tachyzoite cytoskeleton based on previous EM studies (Nichols and Chiappino, 1987) is depicted in Fig. 5 D. At the apical pole, the conoid is associated with the apical polar ring, the IMC, and the sets of 22 pellicular microtubules. The posterior polar ring delineates the termination of the IMC at the rear end of the parasite. A large parasitophorous vacuole containing 32 parasites arranged in rosette illustrates the focused staining at the posterior pole of the parasites, which corresponds to the center of the rosette. A weaker staining at the periphery corresponds to the apical tip of each parasite (Fig. 5 E). The restricted localization of MyoC is unlikely to depend only on direct interactions with actin filaments since the treatment of recombinant parasites with 10 μM cytochalasin D for 2 h did not alter the ring structures visualized by IFA (unpublished data).

The tails of MyoB and MyoC determine their specific localizations

Three distinct domains define the modular structure of most myosins. The catalytic motor domain binds to actin, the regulatory neck region carries the light chains and structurally acts as a lever arm, and the tail domain is responsible for the functional diversity of each molecule. The tail domains appear to contribute predominantly as determiners of subcellular localization; they bring the motor to its site of action. MyoB and

MyoC share a common core region in their tail domain and diverge only in their last 21 and 118 amino acids, respectively. To assess the importance of these domains, we fused GFP to fragments encoding the tails of MyoB or MyoC. Additionally, to examine the efficiency of alternative splicing in tachyzoites, we fused GFP to a genomic fragment of the MyoB/C gene that encompasses both tail exons. Stable clones expressing GFP–Btail, GFP–Ctail, or the GFP–B/Ctail chimera were isolated and characterized. The myc–GFP–Btail and myc–GFP–Ctail fusions showed the expected mobility shift compared with GFP on a Western blot (Fig. 6 F). Interestingly, parasites expressing GFP fused to the genomic fragment of MyoB/C predominantly produced GFP–Ctail. Only a trace of a product comigrating with GFP–Btail was visible. This result correlates with the predominance of MyoC versus MyoB in wild-type tachyzoites (Fig. 2 C) and suggests that a fully processed transcript is the major spliced form (Fig. 3 C). The subcellular localization of GFP–tail fusions was determined by IFA and confocal microscopy. Consistent with the localization of full-length MyoB and MyoC, GFP–Btail was distributed in a punctate pattern throughout the cytoplasm, whereas GFP–Ctail accumulated in ring structures at the extremities of the parasites (Fig. 6, B and C). In parasites undergoing cell division and thus containing two nuclei, two rings are visible and likely correspond to the posterior polar rings of the forming daughter cells (Fig. 6 D, and also Fig. 1, b–d). In perfect agreement with the results of Western blotting, the GFP–B/Ctail fusion was mostly found to localize at the polar rings similar to GFP–Ctail (Fig. 6 A). GFP fused to the last COOH-terminal 118 amino acids of MyoC did not localize to the polar rings but was abundant and diffuse in the cytosol (Fig. 6 E). This result indicates that the determinants of MyoC localization are not restricted to the region specific to MyoC, and additional information in the common core of the two tails is important for the selective targeting.

MyoB is readily soluble, whereas MyoC partitions with the detergent-insoluble fraction

We examined the nature of the interaction between MyoB, MyoC, and other cellular components by biochemical fractionation followed by Western blot analysis. The *T. gondii* catalase has recently been shown to fractionate with the soluble proteins (Ding et al., 2000) and was used here as a marker of complete lysis. Previous analysis had shown that GFP is readily soluble when parasites are lysed in PBS (Hettmann et al., 2000). MyoB mainly partitioned with the soluble fraction, whereas MyoC was resistant to solubilization in the presence of high salt and could not be extracted by detergent (2% Triton X-100). Complete solubilization of MyoC was obtained with carbonate treatment, pH 11.5 (Fig. 7 A). Fractionation in the presence of 2% Triton X-100 and 10 mM ATP released about half of the MyoC (Fig. 7 B). A similar observation has recently been reported for endogenous MyoC (Heintzelman and Schwartzman, 1999). The profile of GFP–MyoCtail solubility was almost identical to the one obtained with full-length MyoC. Indeed, similar to MyoC, GFP–Ctail associated quantitatively with the particulate fraction even in the presence of Triton X-100. However, and in contrast to MyoC, in the presence of detergent and ATP, GFP–Ctail remained insoluble (Fig. 7 B).

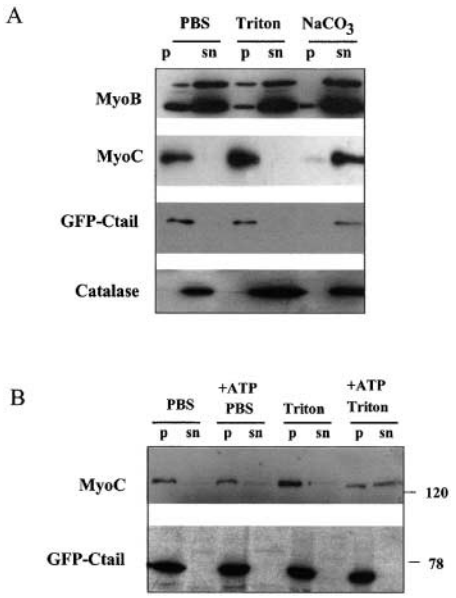

Figure 7. **Distribution of recombinant MyoB and MyoC, studied by subcellular fractionation**. Cells expressing myc–MyoB and myc–MyoC were lysed in the presence or absence of 10 mM ATP under different conditions, and separated by high speed centrifugations into soluble (sn) and particulate (p) fractions. Cells were lysed either in PBS, PBS with 2% Triton X-100, 0.1 M Na_2CO_3 (pH 11.5), or 1 M NaCl. The distribution of myc–MyoB, myc–MyoC, and GFP–Ctail were detected using the anti-myc antibodies. The distribution of endogenous catalase was used as a control and determined simultaneously by immunoblotting with anticatalase polyclonal antibodies.

Parasites overexpressing MyoB harbor morphological defects during cell division

The integration of a second copy of MyoB controlled by the TUB1 promoter led to significant overexpression of MyoB compared with the wild-type situation. In contrast, MyoC was expressed at a level comparable to the endogenous protein (Fig. 2 C). We isolated several independent clones exhibiting variable levels of MyoB expression (Fig. 8 F). In addition to full-length MyoB, clone B1 accumulated notable amounts of a degradation product, mimicking MyoB/CΔtail. Indeed, the truncation corresponds to a large deletion in its tail region, as demonstrated by using antibodies recognizing the NH_2-terminal epitope tag. Upon morphological examination, this clone showed strong phenotypic abnormalities during cell division. By IFA, most vacuoles were shown to contain one or multiple large residual bodies staining for MyoB, but failed to stain with DAPI (Fig. 8 A). The same phenotype was observed with other clones, though with a variable severity. MyoB and actin accumulated significantly in these structures (Fig. 8 B), but they were only weakly stained for rhoptries (unpublished data) or microneme markers (Fig. 8 C). Such residual bodies were most frequently located at the posterior of the parasites, whereas bleb-like protrusions were found distributed more randomly around the parasites. The presence of the glycosyl phosphatidylinositol–anchored plasma membrane marker, SAG1 (Fig. 8 D), around the residual bodies concomitant with the absence of staining with an IMC marker (Fig. 8 E) indicated that

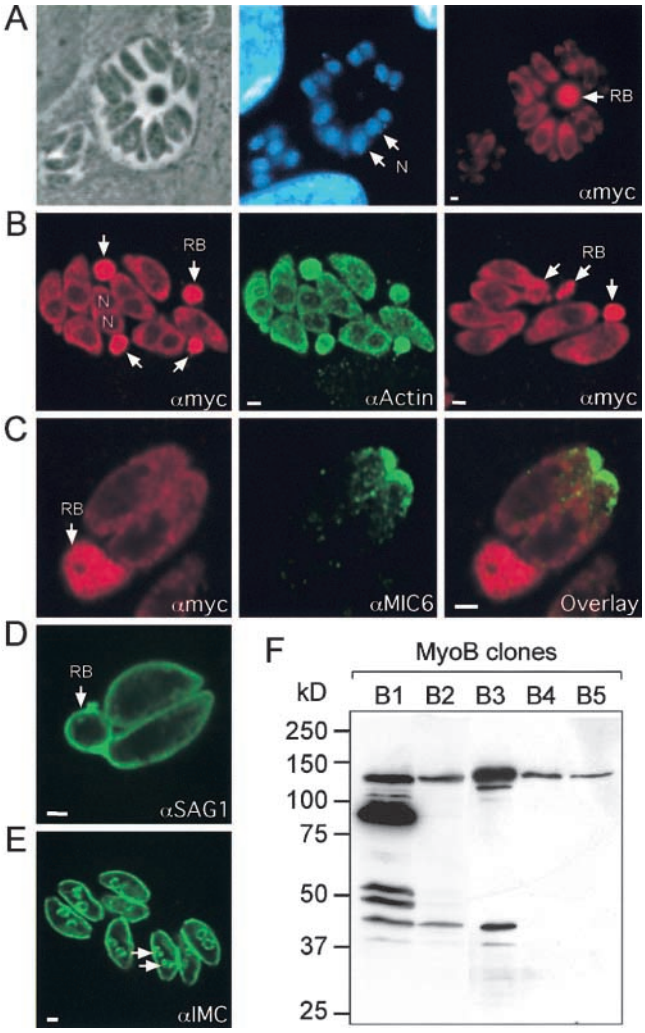

Figure 8. **Phenotypic analysis of parasites overexpressing MyoB.** Detection of residual bodies in intracellular parasites expressing myc–MyoB (clone MyoB/1) by confocal microscopy. (A) The residual bodies detected with anti-myc antibodies did not stain with DAPI. (B) Colocalization of MyoB (polyclonal anti-myc) with actin illustrated their coenrichment in residual bodies. (C) Residual bodies were not significantly stained with the microneme marker anti-TgMIC6. In contrast, they stained with antibodies recognizing the glycosyl phosphatidylinositol–anchored surface antigen SAG1 (D), but were not detected by antibodies recognizing a protein of the IMC (E). The latter marker visualized the high frequency of dividing parasites in the population by detecting the presence of newly formed daughter cell IMCs (E, arrows). (F) Western blot analysis of independent recombinant *T. gondii* clones expressing MyoB at different levels. N, nucleus; RB, residual body. Bars, 1 μm.

these bodies were surrounded solely by the plasma membrane. Numerous vacuoles contained parasites that had not accurately separated, and the geometrical organization in rosettes was rarely seen in the overexpressers compared with wild-type parasites. DAPI and IMC staining revealed an unusual proportion of parasites undergoing cell division (Fig. 8 E, arrows). Quantification at the EM level revealed that the process of cell division was slower in MyoB overexpressers, since more than 40% of the parasite population was in the middle of endodyogeny (two nuclei per cell) compared with less than 10% in wild-type parasites.

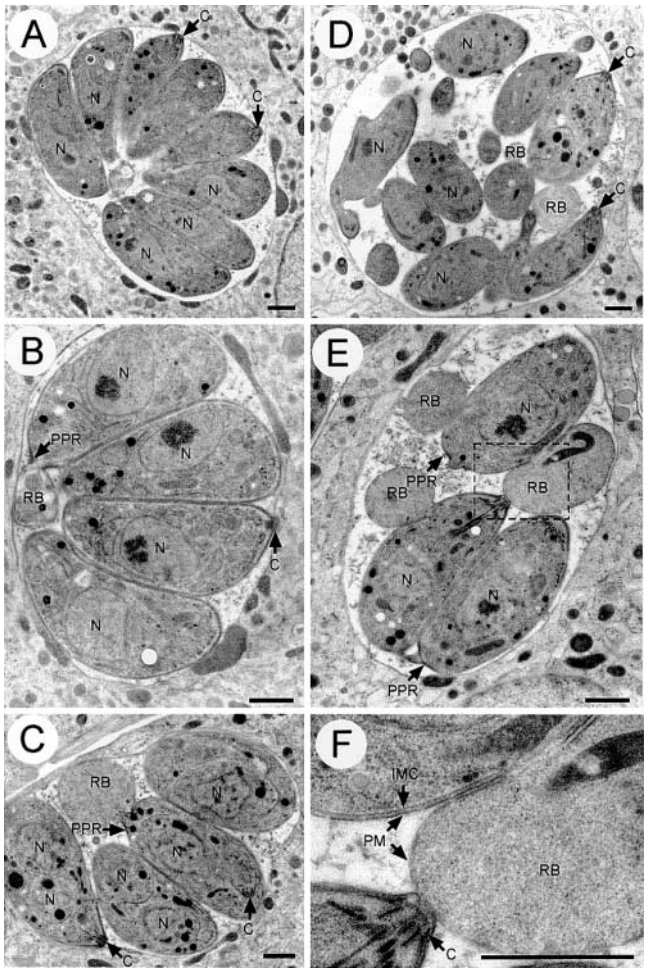

Figure 9. **Ultrastructural analysis of the residual bodies induced by MyoB overexpression.** Thin section electron micrographs of wild-type parasites (A and B) and parasites overexpressing myc–MyoB (C–F). Wild-type parasites divide and form regular rosettes (A and B), whereas the vacuoles of transgenic parasites are highly disorganized (C–E). The boxed region in E is presented at higher magnification in F. Residual bodies are clearly distinguished from parasites, as they lack the IMC and are surrounded only by the plasma membrane (C–F). In wild-type parasites, residual bodies such as the one seen in B were rare. C, conoid; N, nucleus; PM, plasma membrane; PPR, posterior polar ring; RB, residual body. Bars, 1 μm.

Ultrastructural analysis of MyoB overexpressers

Thin section transmission EM of clones overexpressing MyoB revealed severe morphological defects. The MyoB overexpressers showed a significantly disorganized arrangement within the parasitophorous vacuole (Fig. 9, D and E) compared with the regular rosettes formed by wild-type parasites (Fig. 9, A and B). Presence of residual bodies, as observed by light microscopy, was also visible at the EM level. Most of these large cytoplasmic extensions were directly connected to the parasites, and were not only seen at the posterior (Fig. 9 C) but also toward the anterior pole (Fig. 9 E). Higher magnification clearly revealed that the bleb-like bulges were only surrounded by the plasma membrane and the IMC was absent (Fig. 9 F), confirming the data obtained by confocal microscopy (Fig. 8). The quasi absence of organelles in these residual bodies distinguished them from the

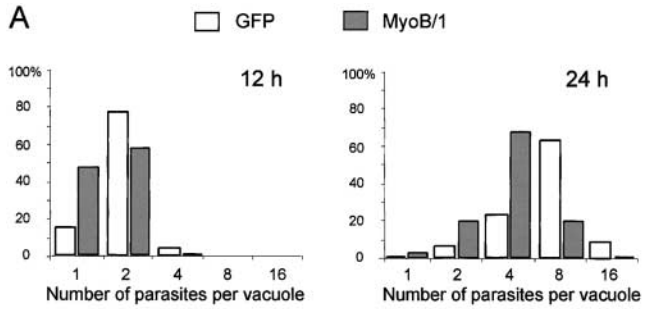

B

T. gondii strains[a]	Survivors[b]	Seropositivity of survivors[c]	Mortality[d]
RH GFP (wild type)	3/15	0/3	100%
RH MyoB/1 overexpresser	21/25	18/21	18%

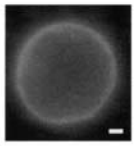

Figure 10. **Overexpression of MyoB delays cell division and reduces virulence in mice.** (A) Parasites expressing GFP or MyoB were allowed to invade host cells at 37°C for 10 min; the cells were then further incubated for 12 and 24 h. For each condition, 100 vacuoles were analyzed, and the number of parasites per vacuole is presented in a histogram. (B) Overexpression of MyoB allowed mice to survive acute infection with *T. gondii* RH. Summary of two independent experiments: a group of five mice was inoculated with the two parasite lines in the first experiment. Groups of 10 mice (RHGFP) and 20 mice (RHMyoB overexpresser) were inoculated per parasite line in the second experiment. (B[a]) The RHMyoB strain was compared with RH expressing GFP. (B[b]) Numerators correspond to the number of surviving mice 4 wk after infection; denominators indicate the total number of mice inoculated in two independent experiments. (B[c]) Numerators represent numbers of surviving mice that were positive for *T. gondii* serology; denominators represent the total number of mice surviving in the two separate experiments. (B[d]) The percentage was corrected according to the real infection rate; the seronegative mice were not taken into account. (C) Isolation of cysts in brains of infected mice 2 mo after intraperitoneal inoculation with mutant parasites overexpressing MyoB. The cysts were stained specifically with the *Dolichos biflorus* FITC–labeled lectin, which recognizes the cell wall of *T. gondii* cysts. Bar, 10 μm.

structures created by treatment with cytochalasin D (Shaw et al., 2000).

MyoB overexpressers showed a delay in cell division and reduced virulence in mice

To assess the influence of stable MyoB overexpression on growth rate, we counted parasites per vacuole at 12 and 24 h after infection. Parasites expressing MyoB exhibited a significant growth delay compared with parasites expressing GFP (Fig. 10 A) and GFP–MyoBtail (unpublished data), suggesting that the motor is necessary for the phenotype. To determine if this mutant exhibits an alteration of virulence in vivo, two series of experiments were conducted with groups of mice infected in the intraperitoneal cavity with 20 parasites of either RH or RHMyoB (Fig. 10 B). As reported previously, the inoculation of wild-type RH is always lethal in mice (Mercier et al., 1998), and all infected (seropositive) mice died within 7 d. In contrast, a large proportion of mice infected with RHMyoB survived the challenge. 2 wk later, the mice were tested for seropositivity to confirm infection. To examine if the attenuated parasites were able to establish a chronic infection in the animal, we searched for the presence of cysts using specific staining with the *Dolichos biflorus* lectin (Boothroyd et al., 1997). The presence of a few cysts per brain was indicative of a chronic infection in all mice analyzed (Fig. 10 C).

Discussion

Cytokinesis is the process by which a cell partitions its surface and cytoplasm to form two daughter cells. In both animal and yeast cells, this process involves the assembly and contraction of an actomyosin ring. It is noteworthy that for a long time, among the hundreds of myosins known, only the conventional myosins of class II had been implicated in cell division (Field et al., 1999). However, a recent study established the involvement of two myosins of type V in *S. pombe* (Win et al., 2001). The asexual multiplication of *T. gondii* occurs by a peculiar process named endodyogeny, which is defined as the gradual development of two daughter parasites within a fully differentiated mother; the mother is incorporated into the daughters during the process (Fig. 1). In *T. gondii*, actin inhibitors did not prevent replication, per se, but disrupted the inheritance of mother cell organelles, resulting in the formation of residual bodies (Shaw et al., 2000). Therefore, myosin motor(s) were anticipated to function in one or several aspects of parasite division. However, the lack of detectable actin filaments in *T. gondii* under physiological conditions (Dobrowolski et al., 1997) has hampered the assignment of a role for actomyosin during furrowing and completion of daughter cell membrane separation.

Parasites treated with BDM, an inhibitor of myosin ATPase, underwent proper nuclear replication but showed impairment in cell division, similar to the cytokinesis defects observed in other organisms (unpublished data). This observation suggested a critical role for a myosin during endodyogeny, but was inconclusive because this drug is known to have pleiotropic targets. Until now, no myosin of class II or V has been identified in Apicomplexa. To assign which myosin could be involved in the cell division process, we examined the pattern of expression and subcellular distribution of the five class XIV myosins identified so far in *T. gondii.* MyoA is the prominent motor candidate for powering parasite gliding motility, whereas MyoE could not be involved because it is not expressed at a detectable level in tachyzoites. We confidently excluded MyoD because disruption of the MyoD gene by homologous recombination did not affect parasite division (unpublished results).

MyoB and MyoC are the products of alternatively spliced transcripts from the same gene (Fig. 3; Heintzelman and Schwartzman, 1997). These two transcripts are present in tachyzoites but are upregulated in bradyzoites. The abundance of the respective myosins suggests that a partial splicing leading to the production of MyoB occurs much less frequently. Thus, MyoC appears to be the predominant product in tachyzoites. This observation was confirmed by the fusion of a GFP coding sequence to a fragment of the MyoB/C gene covering the tail exons, which generates essentially GFP–MyoCtail.

Unexpectedly, MyoB, MyoC, and MyoB/CΔtail (including the motor and a divergent IQ motif) have a dominant effect under conditions of transient expression; this motor does not segregate equally during cell division. There is no obvious explanation for this unusual behavior, but it clearly implies an interaction of the motor with an as yet undefined cellular structure that might fail to segregate properly due to the overexpression or is naturally unevenly distributed between the daughter cells. We speculate that this structure or organelle might be the IMC or part thereof. First, during transient expression, MyoB, MyoC, and even the motor domain truncated of its tail localize to the cell periphery, to punctate structures and patches, as well as to membrane structures that appear to extend between the dividing daughter cells. Second, the almost exclusive localization of MyoC at the termination of the IMC suggests that this myosin might fulfill a direct role in assembly and elongation of this complex during budding of the daughter cells. Indeed, MyoC is associated with the IMC at an early stage of daughter cell formation (Fig. 6 D). This is reminiscent of the situation in *Caenorhabditis elegans* where myosin VI was shown to be required for asymmetric segregation of cellular components during spermatogenesis (Kelleher et al., 2000). The partitioning of MyoC with the detergent-insoluble fraction implies an interaction with components of the parasite cytoskeleton. This posterior structure is not disrupted by treatment with cytochalasin D and thus appears independent of the presence of intact actin filaments. Nevertheless, MyoC was previously shown to be a classical myosin, binding to F-actin in an ATP-sensitive fashion (Heintzelman and Schwartzman, 1999). The analysis of GFP–Ctail fusion confirmed that the localization and sedimentation determinants are confined within its tail domain.

In addition to the segregation defects, transient expression of both MyoB and MyoC leads to the accumulation of residual bodies at the posterior of the parasites after division. Both morphological defects observed during transient expression of MyoC and MyoB/CΔtail could not be analyzed further in stable cell lines because no viable transformant could be obtained with MyoB/CΔtail, and lines only expressing low levels of MyoC were obtained. Overexpression of class I myosins in *Dictyostelium discoideum* has been reported to lead to a phenotype similar to knockout mutants (Novak and Titus, 1997). As the MyoB/C gene is most likely indispensable, we will need to generate a conditional knockout based on an inducible system, which has recently been established for *T. gondii* (Meissner et al., 2001).

Here, stable MyoB overexpression induced a clear defect in proper separation of the daughter cell membranes, although nuclear division and formation of the daughter conoids appeared normal. In addition, the mutant did not show any impairment in host cell invasion (unpublished data), another actomyosin-dependent process proposed to involve MyoA. Generation of large residual bodies at the posterior end of the parasites and the presence of bleb-like structures randomly distributed around the parasites suggest an impairment in endodyogeny. Residual bodies appear to concentrate MyoB and actin but are essentially devoid of organelles and DNA. These bodies are therefore distinct from the residual bodies induced by treatment with actin inhibitors, which were shown to contain rhoptries, micronemes, a part of the mitochondrion, the apicoplast, and some ER (Shaw et al., 2000). The actomyosin system thus seems to play a role late in the division process, after replication, when the IMC (partly of the mother cell, partly formed de novo) slides over the newly formed conoid and microtubule basket of the daughter cells.

MyoC is the best candidate for directly participating late in the division process, as it accompanies the posterior polar ring during its descent through the mother cell, encircling each daughter. This role is reminiscent of the proposed function of myosin VI in the sliding of membranes along the length of the spermatid nuclei and axonemal microtubules during the individualization of syncitial spermatids in *Drosophila* (Hicks et al., 1999). The phenotypic consequences of MyoB overexpression are also suggestive of its role at the end of cell division. In this case, the sliding of the mother plasma membrane onto the IMC of the budding daughter cells does not occur properly and tightly, leading to the creation of plasma membrane blebs. MyoB is associated with the cell periphery and IMC lamellae, suggesting its direct involvement. Additionally, the creation of large residual bodies at the posterior pole are indicative of an improper sealing or closure, a process analogous to the constriction of the cleavage furrow occurring in other eukaryotic cells, which is myosin II dependent. We conclude that both MyoB and MyoC have localizations relevant to parasite division, but the similar phenotype caused by overexpression of MyoB, MyoC, and MyoB/CΔtail is more likely to result from an interference with the function of the predominant product in tachyzoites, MyoC.

Although close homologues of *T. gondii* MyoA can be found in all apicomplexan parasites for which significant DNA sequence information is available, including *Plasmodium*, *Neospora*, *Eimeria*, and *Cryptosporidium* species, there is no evidence for the presence of a myosin closely related to MyoB/C in other apicomplexan parasites thus far. Endodyogeny shares many similarities with the general process of shizogony, the usual asexual multiplication mechanism in Apicomplexa; however, endodyogeny takes place in a fully differentiated mother parasite that keeps its highly sophisticated invasion complex throughout division (Porchet-Hennere et al., 1985). In particular, the IMC, which is composed of Golgi-derived saccules, is maintained in the mother and partly recycled into the daughter cells by a process that is poorly understood. Contrasting to this, in other Apicomplexa such as *Plasmodium*, zoites form de novo at the periphery of a multinucleate, undifferentiated cytoplasmic mass. Therefore, *T. gondii* may have evolved specific ways of integrating old material into new zoites, and because this process is highly dynamic in terms of membrane–cytoskeleton interactions, myosins are likely to be involved.

Finally, whereas intraperitoneal infection with RH is always lethal, impairment in cell division caused by overexpression of MyoB leads to a major reduction in virulence and the formation of cysts in the brain of infected mice. It will be very interesting to examine the ultrastructure of these cysts, but their limited numbers has hampered such analysis so far. These results are very similar to the ones reported for the knockout of the dense granule protein 2 gene (GRA2) in

RH, which led to decreased virulence and chronic infection (Mercier et al., 1998).

Materials and methods

Reagents

Restriction enzymes were obtained from New England Biolabs, Inc. The secondary antibodies were from Bio-Rad Laboratories and Molecular Probes. Mouse ascites fluid of the 9E10 anti-myc hybridoma were used at 1:1,000. The antiactin monoclonal was generated against *D. discoideum* actin. The rabbit polyclonals anticatalase, anti-MIC6, and anti-MyoAtail were used as previously described (Ding et al., 2000; Hettmann et al., 2000; Reiss et al., 2001). Polyclonal antipeptide antibodies were generated as previously described (Hettmann et al., 2000). Peptides: B/C1, aa 304-NVSIEGKDAQGVPDAAYISPQC; B/C2, aa 763-PEEREALLSGMERPRNP; C1, aa 988-MNSKVPPYMQKDVSYLC; C2, aa 1030-GRYSEPFGGAWNVVC.

Growth of parasites and isolation of DNA and RNA

T. gondii tachyzoites (RH strain wild-type and RH hypoxanthine-xanthine-guanine-phosphoribosyltransferase [hxgprt]$^-$) were grown in human foreskin fibroblasts (HFF) maintained in DME with 10% FCS, 2 mM glutamine, and 25 μg/ml gentamicin. Parasites were harvested after host cell lysis and purified by passage through filters with 3.0 μm pores and centrifugation in PBS. Genomic DNA was isolated from purified parasites as previously described (Sibley and Boothroyd, 1992). Total RNAs were prepared using "RNA clean2" (AGS GmbH) according to the manufacturer's instructions.

T. gondii genomic library screening

A clone containing the MyoB/C locus was isolated from a cosmid library made in a SuperCos vector modified with a SAG1/ble *T. gondii* selection cassette. The library (provided by D. Sibley and D. Howe, Washington University, St. Louis, MO) was prepared from a Sau3AI partial digestion of RH genomic DNA ligated into the BamHI cloning site. We partially sequenced the MyoB/C locus (GenBank/EMBL/DDBJ accession number AAF09586). Probes were labeled using DIG-11-dUTP. Hybridization and chemiluminescent CSPD detection were performed according to the manufacturer (Roche Molecular Biochemicals).

Construction of *T. gondii* expression vectors

The MyoB and MyoC coding sequences were amplified by RT-PCR using total RNA from the Prugniaud strain. Both cDNAs were sequenced (GenBank/EMBL/DDBJ accession numbers MyoB, AF438184; MyoC, AF438183). The vectors pTmyc–MyoB and pTmyc–MyoC were generated by cloning the cDNA between NsiI and PacI sites of the pTmyc–GFP-HX vector (Hettmann et al., 2000). The restriction sites PstI and PacI were introduced in the sense primer 1B/C and antisense primer 2B or primer 2C, respectively. Both myosins carry an NH_2-terminal c-myc epitope and 7xHis residues (MQEQKLISEEDLAMAMHHHHHHH) to produce myc–MyoB and myc–MyoC. The vector pTmyc–MyoB/CΔtail was generated by the PCR amplification of a fragment coding for the first 754 amino acids of MyoB/C using primers 1B/C and 2B/C. The myc–GFP–tail fusion vectors were constructed by cloning the tail fragments between PstI and PacI sites of the pTGFP-HX vector. To generate pTGFP–tailB and pTGFP–tailC, the PstI-PacI fragments corresponding to the COOH-terminal tails of MyoB and MyoC were amplified from cDNAs using primers 3B/C and 2B or 3B/C and 2C. A GFP fusion with the last 118 amino acids of MyoC was obtained by PCR amplification using primers 4C and 2C to generate pTGFP–tailCΔ118. A fusion with the genomic sequence of MyoB/C tail was obtained by PCR amplification from a cosmid clone using primers 3B/C and 2C to generate pTGFP–tailB/C. The 3′UTR of MyoB/C was amplified from a cosmid clone using primers 5C and 6C and introduced into pTGFP–tailB/C to replace the 3′ untranslated region (UTR) of SAG1.

Primers:1B/C, 5′-AACTGCAGGACACGCAGCTGGAACTCGAG-3′; 2B, 5′-GCCGGATCCTTAATTAACTATGTTTTTGATTATGTTTCCATGTCAG-3′; 2C, 5′-GCCGGATCCTTAATTAAGGTCTATCCGGCGCACAGGC-3′; 2B/C, 5′-GCCTTAATTAAGATGCATGTCTGCGCGCGTTTGATTCC-3′; 3B/C, 5′-GCCGGATCCGCTGCAGTCCTGGGCCCGATGTGG-3′; 4C, 5′-AACTGCAGGCATTGTGCGCGTCATGAATAGC-3′; 5C, 5′-CCTTAATTAACCTTTAAAGTGGACAAGGGTGA-3′; 6C, 5′-GCCGGATCCAGGACGGTAGTGGTCGGG-3′.

Parasite transfection and selection of stable transformants

T. gondii tachyzoites (RHhxgprt$^-$) were transfected by electroporation as previously described (Soldati and Boothroyd, 1993). The HXGPRT was used as a positive selectable marker in the presence of mycophenolic acid and xanthine as previously described (Donald et al., 1996).

Western analysis of parasite lysates

Crude extracts of tachyzoites were separated by SDS-PAGE (Laemmli, 1970). Western blot analysis was performed essentially as described by Soldati et al. (1998) using 8–10% polyacrylamide gels run under reducing conditions, followed by transfer to Hybond ECL nitrocellulose. For detection, affinity-purified, HRP-conjugated goat anti–mouse IgG or goat anti–rabbit IgG (1:2,000) and the ECL system (Amersham Pharmacia Biotech) were used. Direct recording of chemoluminescent signals and densitometry by the Luminescent Image Analyzer LAS-1000 (FujiFilm) allowed for quantification of signal intensities within a broad linear range.

Cell fractionation

10^9 parasites, freshly released from infected cells, were resuspended in 1 ml of bufffer (either PBS, PBS/1 M NaCl, PBS/0.1 M Na_2CO_3 (pH 11.5), or PBS/2% Triton X-100) and lysed by sonication (four times, 30 s each; on ice). 10 mM ATP was freshly added to minimize the interaction of the myosin with F-actin. Pellet and soluble fractions were separated by ultracentrifuging for 1 h at 55,000 rpm at 4°C.

Indirect immunofluorescence microscopy and detection of GFP in *T. gondii*

All manipulations were performed at room temperature. Intracellular parasites grown in HFF on glass slides were fixed with 4% paraformaldehyde and 0.05% glutaraldehyde for 20 min. After fixation, slides were rinsed in PBS/0.1 M glycine. Cells were then permeabilized in PBS/0.2% Triton X-100 for 20 min and blocked in the same buffer with 2% FCS. Slides were incubated for 60 min with primary antibodies diluted in PBS/1% FCS, washed, and incubated for 60 min with Alexa488- or FITC-labeled goat anti–mouse IgGs diluted in PBS/1% FCS. Rapid freezing in ultra cold methanol with combined fixation/permeabilization was performed as described by Neuhaus et al. (1998). Slides were mounted in Vectashield and kept at 4°C in the dark. Intracellular parasites expressing GFP were fixed according to the above protocol and mounted immediately. Confocal images were collected with a Leica laser scanning confocal microscope (TCS-NT DM/IRB) using a 100× Plan-Apo objective with NA 1.30. Single optical sections were recorded with an optimal pinhole of 1.0 and 16 times averaging**.** All other micrographs were obtained on a Zeiss Axiophot with a camera (Photometrics Type CH-250). Adobe Photoshop and Canvas 7 were used for image processing.

EM

HFF cells were plated on sapphire coverslips for 3 d before infection with parasites. Then, the coverslips were plunged into an ethane slush at −170°C, freeze substituted, and embedded in Lowicryl as previously described (Neuhaus et al., 1998). Sections were observed and documented on a Philips 400 T TEM. The EM negatives were scanned at 1,200 dpi and imported into Adobe Photoshop for processing.

In vivo experiments

BALB-c mice were inoculated by intraperitoneal injection of 20 freshly harvested tachyzoite parasites from the wild-type RH strain or with MyoB-overexpressing RH. 3 wk after infection, the number of survivors was recorded and their *T. gondii* serology was tested by Western blotting against an RH tachyzoite lysate.

Isolation of *T. gondii* cysts from the brain of infected mice

Seropositive mice survivors were killed 8 wk after intraperitoneal injection of 20 parasites from MyoB-expressing RH. Parasite cysts were isolated from the brain as previously described (Tomavo et al., 1991). The cyst preparation was incubated for 1 h with the FITC-labeled lectin from *Dolichos biflorus,* diluted 1:50, at 37°C.

We are grateful to Dr. J.F. Dubremetz (UMR CNRS 5539, Montpellier, France) for his assistance during earlier stages of the project and the critical discussions. We thank Dr. G. Ward and K.L. Carey (University of Vermont, Burlington, VT) for providing us with the mAb 45.15 recognizing a 70-kD protein of the IMC.

This work was funded by the Deutsche Forschungsgemeinschaft (DFG grant SO 366/1-1, SO366/1-2) and The Biotechnology and Biological Sciences Research Council. Dr. F. Delbac was supported by a grant of the Von Humboldt foundation. E. Neuhaus was a recipient of a postdoctoral fellowship from the Max Planck Society.

Submitted: 28 December 2000
Revised: 28 September 2001
Accepted: 5 October 2001

References

Ajioka, J.W., J.C. Boothroyd, B.P. Brunk, A. Hehl, L. Hiller, I.D. Manger, G.C. Overton, M. Marrra, D. Roos, K.-L. Wan, et al. 1998. Gene discovery by EST sequencing in *Toxoplasma gondii* reveals sequences restricted to the Apicomplexa. *Genome Res.* 8:18–28.

Bezanilla, M., J.M. Wilson, and T.D. Pollard. 2000. Fission yeast myosin-II isoforms assemble into contractile rings at distinct times during mitosis. *Curr. Biol.* 10:397–400.

Boothroyd, J.C., M. Black, S. Bonnefoy, A. Hehl, L.J. Knoll, I.D. Manger, E. Ortega-Barria, and S. Tomavo. 1997. Genetic and biochemical analysis of development in *Toxoplasma gondii*. *Philos. Trans. R. Soc. Lond. B Biol. Sci.* 352: 1347–1354.

Ding, M., C. Clayton, and D. Soldati. 2000. *Toxoplasma gondii* catalase: are there peroxisomes in *Toxoplasma*? *J. Cell Sci.* 113:2409–2419.

Dobrowolski, J., and L.D. Sibley. 1997. The role of the cytoskeleton in host cell invasion by *Toxoplasma gondii*. *Behring Inst. Mitt.* 99:90–96.

Dobrowolski, J.M., and L.D. Sibley. 1996. *Toxoplasma* invasion of mammalian cells is powered by the actin cytoskeleton of the parasite. *Cell.* 84:933–939.

Dobrowolski, J.M., I.R. Niesman, and L.D. Sibley. 1997. Actin in the parasite *Toxoplasma gondii* is encoded by a single copy gene, ACT1, and exists primarily in a globular form. *Cell Motil. Cytoskeleton.* 37:253–262.

Donald, R., D. Carter, B. Ullman, and D.S. Roos. 1996. Insertional tagging, cloning, and expression of the *Toxoplasma gondii* hypoxanthine-xanthine-guanine phosphoribosyltransferase gene. Use as a selectable marker for stable transformation. *J. Biol. Chem.* 271:14010–14019.

Field, C., R. Li, and K. Oegema. 1999. Cytokinesis in eukaryotes: a mechanistic comparison. *Curr. Opin. Cell Biol.* 11:68–80.

Goode, B.L., D.G. Drubin, and G. Barnes. 2000. Functional cooperation between the microtubule and actin cytoskeletons. *Curr. Opin. Cell Biol.* 12:63–71.

He, C.Y., M.K. Shaw, C.H. Pletcher, B. Striepen, L.G. Tilney, and D.S. Roos. 2001. A plastid segregation defect in the protozoan parasite *Toxoplasma gondii*. *EMBO J.* 20:330–339.

Heintzelman, M.B., and J.D. Schwartzman. 1997. A novel class of unconventional myosins from *Toxoplasma gondii*. *J. Mol. Biol.* 271:139–146.

Heintzelman, M.B., and J.D. Schwartzman. 1999. Characterization of myosin-A and myosin-C: two class XIV unconventional myosins from *Toxoplasma gondii*. *Cell Motil. Cytoskeleton.* 44:58–67.

Heintzelman, M.B., and J.D. Schwartzman. 2001. Myosin diversity in Apicomplexa. *J. Parasitol.* 87:429–432.

Hettmann, C., A. Herm, A. Geiter, B. Frank, E. Schwarz, T. Soldati, and D. Soldati. 2000. A dibasic motif in the tail of a class XIV apicomplexan myosin is an essential determinant of plasma membrane localization. *Mol. Biol. Cell.* 11:1385–1400.

Hicks, J.L., W.M. Deng, A.D. Rogat, K.G. Miller, and M. Bownes. 1999. Class VI unconventional myosin is required for spermatogenesis in *Drosophila*. *Mol. Biol. Cell.* 10:4341–4353.

Kelleher, J.F., M.A. Mandell, G. Moulder, K.L. Hill, S.W. L'Hernault, R. Barstead, and M.A. Titus. 2000. Myosin VI is required for asymmetric segregation of cellular components during *C. elegans* spermatogenesis. *Current Biol.* 10:1489–1496.

Kepka, O., and E. Scholtyseck. 1970. Weitere untersuchungen der feinstruktur von *Frenkelia* species (M-Organismus, Sporozoa). *Protistologica.* 6:249–366.

Laemmli, U.K. 1970. Cleavage of structural protein during the assembly of the head of bacteriophage T4. *Nature.* 227:680–685.

Meissner, M., S. Brecht, H. Bujard, and D. Soldati. 2001. Modulation of myosin A expression by a newly established tetracycline repressor–based inducible system in *Toxoplasma gondii*. *Nucleic Acids Res.* In press.

Mercier, C., D.K. Howe, D. Mordue, M. Lingnau, and L.D. Sibley. 1998. Targeted disruption of the GRA2 locus in *Toxoplasma gondii* decreases acute virulence in mice. *Infect. Immun.* 66:4176–4182.

Morrissette, N.S., J.M. Murray, and D.S. Roos. 1997. Subpellicular microtubules associate with an intramembranous particle lattice in the protozoan parasite *Toxoplasma gondii*. *J. Cell Sci.* 110:35–42.

Neuhaus, E.M., H. Horstmann, W. Almers, M. Maniak, and T. Soldati. 1998. Ethane-freezing/methanol-fixation of cell monolayers: a procedure for improved preservation of structure and antigenicity for light and electron microscopies. *J. Struct. Biol.* 121:326–342.

Nichols, B.A., and M.L. Chiappino. 1987. Cytoskeleton of *Toxoplasma gondii*. *J. Protozool.* 34:217–226.

Novak, K.D., and M.A. Titus. 1997. Myosin I overexpression impairs cell migration. *J. Cell Biol.* 136:633–647.

Pinder, J.C., R.E. Fowler, A.R. Dluzewski, L.H. Bannister, F.M. Lavin, G.H. Mitchell, R.J. Wilson, and W.B. Gratzer. 1998. Actomyosin motor in the merozoite of the malaria parasite, *Plasmodium falciparum*: implications for red cell invasion. *J. Cell Sci.* 111:1831–1839.

Pinder, J.C., R.E. Fowler, L.H. Bannister, A.R. Dulzewski, and G. Mitchell. 2000. Motile systems in malaria merozoites: how is the red blood cell invaded? *Parasitol. Today.* 16:240–245.

Porchet-Hennere, E., E. Vivier, and G. Torpier. 1985. Origin of membranes of toxoplasma. *Ann. Parasitol. Hum. Comp.* 60:101–110.

Reiss, M., N. Viebig, S. Brecht, M.-N. Fourmaux, M. Soete, M. Di Cristina, J.F. Dubremetz, and D. Soldati. 2001. Identification and characterization of an escorter for two secretory adhesins in *Toxoplasma gondii*. *J. Cell Biol.* 152: 563–578.

Robinson, D.N., and J.A. Spudich. 2000. Towards a molecular understanding of cytokinesis. *Trends Cell. Biol.* 10:228–237.

Shaw, M.K., H.L. Compton, D.S. Roos, and L.G. Tilney. 2000. Microtubules, but not actin filaments, drive daughter cell budding and cell division in *Toxoplasma gondii*. *J. Cell Sci.* 113:1241–1254.

Sibley, L.D., and J.C. Boothroyd. 1992. Construction of a molecular karyotype for *Toxoplasma gondii*. *Mol. Biochem. Parasitol.* 51:291–300.

Soldati, D., and J.C. Boothroyd. 1993. Transient transfection and expression in the obligate intracellular parasite *Toxoplasma gondii*. *Science.* 260:349–352.

Soldati, D., A. Lassen, J.F. Dubremetz, and J.C. Boothroyd. 1998. Processing of *Toxoplasma* ROP1 protein in nascent rhoptries. *Mol. Biochem. Parasitol.* 96: 37–48.

Tilney, L.G., and M.S. Tilney. 1996. The cytoskeleton of protozoan parasites. *Curr. Opin. Cell Biol.* 8:43–48.

Tomavo, S., B. Fortier, M. Soete, C. Ansel, D. Camus, and J.F. Dubremetz. 1991. Characterization of bradyzoite-specific antigens of *Toxoplasma gondii*. *Infect. Immun.* 59:3750–3753.

Vivier, E., and A. Petitprez. 1969. The outer membrane complex and its development at the time of the formation of daughter cells in *Toxoplasma gondii*. *J. Cell Biol.* 43:329–342.

Win, T.Z., Y. Gachet, D.P. Mulvihill, K.M. May, and J.S. Hyams. 2001. Two type V myosins with nonoverlapping functions in the fission yeast *Schizosaccharomyces pombe*: Myo52 is concerned with growth polarity and cytokinesis, Myo51 is a component of the cytokinetic actin ring. *J. Cell Sci.* 114:69–79.

Yahiaoui, B., F. Dzierszinski, A. Bernigaud, C. Slomianny, D. Camus, and S. Tomavo. 1999. Isolation and characterization of a subtractive library enriched for developmentally regulated transcripts expressed during encystation of *Toxoplasma gondii*. *Mol. Biochem. Parasitol.* 99:223–235.